Theor Chim Acta (1997) 95: 201–213

Theoretica Chimica Acta

© Springer-Verlag 1997

Theoretical study of thermal decomposition of azomethane

Imrich Vrábel, Stanislav Biskupič, Andrej Staško

Department of Physical Chemistry, Slovak Technical University, Radlinského 9, 812 37 Bratislava, Slovak Republic

Received May 28, 1996/Final version received November 1, 1996/Accepted November 1, 1996

Summary. Thermal one- and two-bond dissociation processes of *cis*- and *trans*-azomethane were studied by *ab initio* computation with DZP and TZ2P basis sets, using the d(N–C) bond lengths as the reaction coordinates. The geometries were optimized at the MP2 level, and the dissociation energies obtained exploiting a single-point, fourth-order Møller–Plesset calculations [MP4SDTQ/TZ2P]. At this level of theory including zero-point energies, the *trans*-isomer is by 9.3 kcal/mol more stable than the *cis*-isomer. The results show that the energetically more favourable one-bond cleavage proceeds without transition state with the predicted bond dissociation energy D_0 of 47.8 kcal/mol for *trans*-azomethane and 38.5 kcal/mol for *cis*-azomethane. With calculated barrier heights the unimolecular dissociation rate constants have been determined by means of the RRKM theory. The second-order saddle points localized for synchronous decomposition pathways lie 13 (*trans*)-23(*cis*) kcal/mol above the one-bond dissociation energies [MP2/DZP].

Key words: Azomethane – Thermal decomposition – RRKM rate constants – CVTST – Synchronous and asynchronous pathways

1 Introduction

The mechanism of thermal decomposition of azo compounds R–N=N–R has been the subject of considerable attention [1]. The fundamental question is, whether the reaction generally proceeds as a concerted two-bond cleavage (1) or whether the decomposition mechanism involves two separate steps (2):

$$R^1\text{–}N{=}N\text{–}R^2 \rightarrow [R^1\text{–}N{=}N\text{–}R^2]^2 \rightarrow R^{2\cdot} + N_2 + R^{2\cdot}, \quad (1)$$

$$R^1\text{–}N{=}N\text{–}R^2 \rightarrow R^1\text{–}N{=}N^{\cdot} + R^{2\cdot} \rightarrow R^{1\cdot} + N_2 + R^{2\cdot}. \quad (2)$$

Some 70 years ago Ramsperger [2] recognized for the first time that acyclic azoalkanes could eliminate nitrogen by either one or two C–N bond scission in the rate-determining step. Since then countless theoretical and experimental studies were carried out in an attempt to explain the mechanism of thermal decomposition of azo compounds.

Azomethane is one of the most frequently applied azoalkanes in these experiments. The thermal and photochemical decomposition of this compound has been a subject of numerous experimental investigations [3–6]. Practically in every case, the examination was focused on the possible role of bound methyldiazenyl radical in the unimolecular dissociation of azomethane. A time-resolved coherent anti-Stokes Raman scattering (CARS) study [3] on azomethane photodissociation in a gas-phase collisional environment deduced that the methyldiazenyl radical persists as a reaction intermediate for 5 ns before fragmenting into $CH_3^{\cdot}$ and N_2. Recently, a molecular beam investigation [4] deduced a shorter lifetime for the methyldiazenyl radical based on the anisotropy of photofragment angular distributions. Although in these studies the asynchronous dissociation pathway (2) was preferred, the short lifetime of methyldiazenyl radical renders the interpretation of these experiments uncertain.

In spite of the fact that the thermal dissociation of symmetric azoalkanes in gas phase has not been satisfactorily explained, only a few quantum chemical studies were reported up to now for decomposition mechanisms of azo compounds. Dannenberg and Rocklin [7] used the MNDO method with 2×2 CI to study the thermal decomposition of azoethane. It was shown that the activation barriers of two-bond homolysis for both *cis*- and *trans*-azoethane are about 25 kcal/mol higher than the activation barriers of one-bond homolysis. Dannenberg and Rocklin also suggested that the most probable reaction path for the breaking of the C–N bond in azoethane is via the *cis* transition state.

Sole work which employed dissociation of azomethane with inclusion of correlation effects comes from Schaeffer and co-workers [8]. They computed the reaction barriers for synchronous and asynchronous pathways by using CC-SD(T) and TCSCF-CISD methods. They concluded that although in general the agreement was good, the comparison of experiment and theory indicated that the computed barrier heights were underestimated.

Our purpose in the present work was to obtain better agreement with experiment and to calculate rate constants using CVTST (canonical variational transition-state theory). Because the theoretical results underestimate the experimental activation energies and overestimate the rate constants, we describe several ways to improve the potential curve in order to refine the values of the rate constants to better fit the experiment. In particular, we analyzed the influence of the correlation energy, the spin projection, the basis set superposition error and different procedures to scale the reaction path.

2 Computational methods

The calculations have been performed using the GAUSSIAN92 [9] program and all geometries were optimized by the Berny optimization method [10]. Gradients and force constants were determined via analytic techniques at the SCF [11] and correlated levels. The resulting stationary points were confirmed to be the energy minima by the eigenvalues of their Hessian matrices. As a rule for the barrier calculations, it is necessary to include the electron correlation effects. We choose the unrestricted Møller–Plesset perturbation theory, which provides results that are size consistent. It is well-known that the unrestricted Møller–Plesset perturbation theory with spin annihilation is a convenient method to compute potential energy curve for bond dissociation [12], since this method approaches the correct dissociation limit. It has also been reported that PMP4 (projected MP4) results are

comparable in accuracy to those of full CI methods [13]. We used the UHF preoptimized structures as starting points for full geometry searches performed at the UMP2/DZP level. Again, similarly to UHF level, the Hessian matrix calculations confirmed the identities of the basis set to TZ2P at the UMP2 level and reoptimization led to very minor further geometry changes. In the next step, we calculated the energies of these refined structures using the PMP4 method and a TZ2P basis. In addition to the calculation of the CVTST rate constant for the *trans*-azomethane, we determined the minimum energy path (MEP) for asynchronous dissociation pathway. Along this MEP the reaction coordinate was defined as $r = R - R_e$ where R is the d(N–C) distance and R_e is the d(N–C) bond length in equilibrium.

The stability of the wave function was tested using single-excitation configuration interaction (stability test available in GAUSSIAN92) [14]. The wave function was found to be stable with respect to perturbation from excited configurations. The basis sets used in the present study are the DZP (Huzinaga–Dunning) [15] and the TZ2P (Huzinaga–Dunning) [16], with pure d functions (i.e. five d functions).

3 Results and discussion

3.1 Geometries

In both (*cis*- and *trans*-) isomers of azomethane, the methyl groups can assume three possible positions, namely the "staggered" (where the dihedral angles of hydrogens with regard to plane of molecule are 60, −60 and 180), "eclipsed" (0, 120, −120) and "gauche" (−30, 90, 150). It was established in the earlier works [17, 18] that for the *cis* (*trans*) isomer the S–S (E–E) conformer is the most stable. Therefore, we take into account only these conformers in the geometry optimization. The numbering scheme for the *cis*- and *trans*-azomethane and also for reaction products is shown in Fig. 1. Total energies and geometrical parameters for the equilibrium structures are summarized in Tables 1 and 2 (all obtained within the calculated DZP and TZ2P basis sets on the UHF and MP2 levels of theory). These geometrical parameters, calculated at UHF level are in good agreement with the UHF results of Schaeffer et al. [8]. Only a negligible difference for d(N=N) bond length was found. The discrepancies in the geometrical parameters at the correlated levels are the consequence of the differences in the used approximations (MP2 and CISD).

The comparison of geometrical parameters calculated with different basis sets within given level showed that extension of the basis set from DZP to TZ2P has only a small influence on the equilibrium structures. The inclusion of correlation effect into the geometry optimization treatment produces the largest influences on the d(N=N) and d(C–N) bond lengths. Within the more exact MP2 level the R(N–N) bond length is elongated by 0.04 Å for *trans* isomer and by 0.03 Å for *cis* isomer according to the UHF results. The C–N bonds do not display such excess elongation, but are elongated roughly by 0.01 Å on the MP2 level as compared to the original UHF lengths. Summarizing, we have established that the predicted geometrical parameters at the correlated level are in reasonable agreement with experimental data. Two sets of experimental geometrical parameters available for *trans*-azomethane differ significantly only in the a(N–N–C) bond angle. The experimental predictions for this parameter of 119° and 112.3° have been reported using RTG analysis [19] and electron diffraction [20], respectively. Our

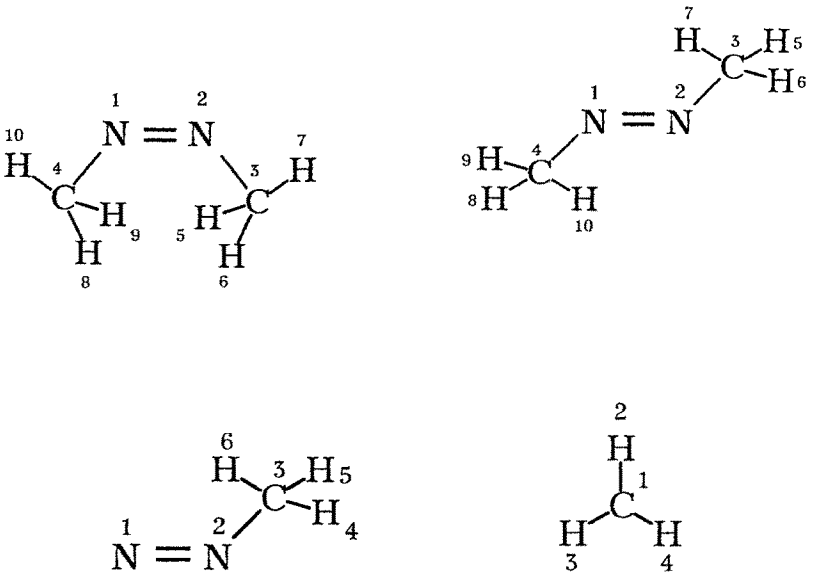

Fig. 1. Numbering scheme for reactants (*cis*- and *trans* azomethane) and products (methyldiazenyl and methyl radical). A complete list of geometrical parameters is summarized in Tables 2 and 6

Table 1. Total energies (in hartrees) for the *cis*- and *trans*-azomethane and the products CH_3N_2 and CH_3

	cis	*trans*	CH_3N_2	CH_3
UHF/DZP	−188.037498	−188.057741	−148.483521	−39.514125
UHF/TZ2P	−188.101625	−188.119836	−148.508298	−39.555997
UMP2/DZP	−188.655594	−188.671971	−148.700935	−39.889139
UMP2/TZ2P	−188.6949680	−188.710675	−148.736715	−39.894773
UMP4/TZ2P	−189.376707	−189.391603	−149.031247	−40.278711

calculations prefer the structure with the lower bond angle, which results in the difference between *cis* and *trans* bond angles of about 7°. This discrepancy can be ascribed primarily to the steric repulsion of methyl groups. It is evident from geometrical parameters that *trans*-azomethane in its ground state has a C_{2h} symmetry within all used theoretical treatments. In contrast with the *trans*-azomethane, the optimized equilibrium geometry of *cis*-azomethane displays an unexpected distortion from C_{2v} symmetry at the UHF level with DZP basis set. A similar phenomenon has been observed by Schaeffer and co-workers [8]. This distortion was not observed for the TZ2P basis set at the same level. The more precise MP2 calculations showed also the C_{2v} symmetry of *cis*-azomethane.

3.2 Frequencies

The UHF and MP2 vibrational analysis performed at the optimized geometries gives the set of harmonic frequencies listed in Tables 3 and 4. These calculated data

Table 2. Predicted equilibrium geometrical parameters for *cis*- and *trans*-azomethane with bond lengths in angstroms and bond angles in degrees

	UHF		UMP2		Experiment	
	DZP	TZ2P	DZP	TZ2P		
trans						
R_{12}	1.213	1.216	1.254	1.242	1.254[a]	1.247[b]
R_{23}, R_{14}	1.448	1.454	1.461	1.465	1.474	1.482
R_{35}, R_{36}, R_{48}, R_{49}	1.089	1.085	1.101	1.102	1.107	1.105
R_{37}, R_{410}	1.088	1.085	1.104	1.104	1.107	1.105
a_{123}, a_{412}	114.1	113.6	112.6	113.3	119.0	112.3
a_{532}, a_{632}, a_{841}, a_{941}	108.3	108.5	108.0	107.9	109.4	107.5
a_{732}, a_{1041}	112.0	111.9	112.1	112.4	109.4	107.5
cis						
R_{12}	1.227	1.235	1.251	1.243	1.254[c]	
R_{23}, R_{14}	1.459	1.462	1.478	1.484	1.480	
R_{35}, R_{36}, R_{48}, R_{49}	1.091 1.089[d]	1.092	1.114	1.105	1.085	
R_{37}, R_{410}	1.085	1.088	1.110	1.097	1.085	
a_{123}, a_{412}	120.8	119.6	120.8	120.2	119.3	
a_{532}, a_{632}, a_{841}, a_{941}	110.9 112.3[d]	110.7	110.1	110.9	109.5	
a_{732}, a_{1041}	107.5	107.9	107.8	107.9	109.5	

[a] Ref. [28], [b] Ref. [27]; [c] Ref. [25]; [d] Symmetry breaking
R_{ij} – Distance between atoms i and j (bond lengths)
a_{ijk} – Angle between atoms i, j and k (bond angles)

were compared with the experimental frequencies reported by several authors. As discussed in Ref. [8], the UHF calculations overestimate the experimental frequencies [21–25] by about 10%. Generally, a good agreement with experiment was obtained after scaling of the UHF vibrational frequencies by the factor of 0.9 was done as suggested by Pople et al. [26], although some modes show large deviations. The largest deviation was in the case of the lowest torsional modes [$\omega_{12}(B_g)$, $\omega_{16}(A_u)$ for *trans*-isomer and $\omega_{12}(B_1)$, $\omega_{17}(A_2)$ for *cis*-isomer], which were underestimated by 50–60 cm^{-1}. It is noticeable that from stretch modes only the $\omega_3(A_g)$ mode for *trans*-isomer and $\omega_3(A_1)$ for *cis*-isomer, which correspond to the N=N stretch, depart from experiments. In their occurrence the weighted values were underestimated by about 140–160 cm^{-1}. This deviation probably follows from the double character of the N=N bond, in which case the correlation effects are required for better description. Indeed, after the weighting of the MP2 vibrational frequencies by 0.94 the discrepancies were significantly smaller with exception of $\omega_{17}(A_2)$ for *cis*-azomethane. We conclude that calculated harmonic vibrational frequencies are insensitive to the basis sets employed in this work within the given level. The largest deviation was 98 cm^{-1} for the UHF level, but for the other modes these differences were less than 30 cm^{-1}.

3.3 Synchronous pathways

In this study, a UHF-based wave function was chosen for the description of the synchronous pathways, because (in innumerable cases) the biradicaloid

Table 3. Predicted vibrational frequencies (in cm^{-1}) and zero-point energies (in hartrees) for *trans*-azomethane

		UHF		UMP2		Experiment[a]
		DZP	TZ2P	DZP	TZ2P	
A_g	ω_1	3280	3254	3184	3165	2989
	ω_2	3182	3170	3135	3148	2926
	ω_3	1589	1606	1627	1642	1583
	ω_4	1584	1601	1497	1521	1437
	ω_5	1433	1335	1472	1476	1381
	ω_6	1342	1395	1253	1241	1179
	ω_7	994	984	1007	985	919
	ω_8	641	638	622	628	591
B_g	ω_9	3263	3263	3181	3174	2977
	ω_{10}	1554	1595	1508	1492	1416
	ω_{11}	1150	1147	1113	1084	1027
	ω_{12}	154	150	198	212	214
A_u	ω_{13}	3263	3236	3184	3179	2981
	ω_{14}	1585	1601	1523	1507	1440
	ω_{15}	1237	1242	1184	1182	1111
	ω_{16}	309	307	322	327	312
	ω_{17}	218	213	236	234	222
B_u	ω_{18}	3280	3254	3184	3166	2988
	ω_{19}	3180	3168	3134	3148	2925
	ω_{20}	1586	1604	1532	1524	1447
	ω_{21}	1540	1565	1481	1482	1384
	ω_{22}	1242	1246	1189	1186	1112
	ω_{23}	1141	1136	1053	1064	1008
	ω_{24}	375	375	372	363	353
ZPE		0.089153	0.088965	0.086808	0.0867908	

[a] Refs. [29–31]

character of molecules has often been properly written down during decomposition [27, 28].

The synchronous transition states were in the first step searched at the UHF/DZP level of theory for both *cis*- and *trans*-isomer, respectively. These transition states were obtained by symmetric elongation of either d(N–C) bond length, where other geometrical constraints were not applied. This careful search led to the maximum on the synchronous reaction pathway. For these stationary points we calculated the vibrational frequencies, from which two were imaginary, corresponding to symmetric and asymmetric C–N stretching modes. The geometries, obtained in this way, were used to the search for the second-order saddle points both UHF and MP2 levels. The results of these calculations are summarized in Table 5. In every case the transition structures maintain the C_{2v} or C_{2h} symmetry, respectively. The d(C–N) distances of approximately 2.25 Å are very long relative to the distances 1.45 Å in equilibrium structures. The comparable small values of the imaginary vibrational frequencies reflect a broad potential barrier for the synchronous mechanism. The comparison of our barrier heights with the

Table 4. Predicted vibrational frequencies (in cm^{-1}) and zero-point energies (in hartrees) for *cis*-azomethane

		UHF		UMP2		Experiment	
		DZP[c]	TZ2P	DZP	TZ2P		
A_1	ω_1	3310	3286	3197[b]	3164	3006[a]	3006[b]
	ω_2	3243	3231	3112	3126	2902	2904
	ω_3	1592	1571	1618	1623	1556	1561
	ω_4	1563	1598	1534	1521	1438	1438
	ω_5	1486	1413	1495	1476	1373	1370
	ω_6	1217	1234	1167	1153	1088	1087
	ω_7	973	958	935	932	862	861
	ω_8	426	407	438	426	398	398
B_1	ω_9	3251	3223	3188	3181	2956	2960
	ω_{10}	1639	1686	1531	1543	1465	1460
	ω_{11}	1048	1052	1074	1068	997	935
	ω_{12}	148	163	182	174	165	?
A_2	ω_{13}	3267	3258	3163	3147	2975	2960
	ω_{14}	1608	1597	1559	1540	1466	1479
	ω_{15}	1254	1281	1235	1238	1179	1170
	ω_{16}	481	494	507	494	464	464
	ω_{17}	86	24	72	115	220	242
B_2	ω_{18}	3267	3258	3166	3147	2974	3019
	ω_{19}	3238	3233	3124	3131	2912	2920
	ω_{20}	1639	1686	1530	1543	1465	1430
	ω_{21}	1448	1442	1428	1426	1350	1359
	ω_{22}	1292	1298	1203	1214	1161	1159
	ω_{23}	1102	1086	1061	1050	956	935
	ω_{24}	682	674	662	657	623	625
ZPE		0.088604	0.0883912	0.086204	0.086177		

[a] Ref. [33]; [b] Ref. [32]; [c] Symmetry breaking

results published in Ref. [8], which were calculated by TCSCF-CISD method, leads to the interesting facts. Whilst the TCSCF method gives for both reaction pathways approximately similar energy barriers, the UHF wave function assumes about 10.6 kcal/mol higher barrier for *trans* synchronous pathway. This discrepancy reflects the fact that the UHF wave function probably does not describe exactly the synchronous decomposition pathway, although the above results are qualitatively the same as the predictions of Schaeffer et al. (see Table 5).

We did not find the saddle point with one imaginary vibrational frequency only, which could correspond to a two-bond cleavage. The obtained results indicate that the gas-phase decomposition of azomethane by synchronous mechanism is unfavourable not only from energetical point of view, but in our opinion such reaction pathway with true transition state probably does not exist.

3.4 Asynchronous pathway

In an asynchronous pathways both *cis*- and *trans*-azomethane decompose into methyldiazenyl and methyl radicals. In order to find the transition structure,

Table 5. Total energies (in hartrees), zero-point energies (in hartrees), imaginary frequencies (in cm^{-1}) d(N–C) bond lengths (in angstroms) and barrier heights (in kcal/mol) for *cis*- and *trans* synchronous transition states

Properties	*trans*		*cis*	
Method	UHF-DZP	UMP2-DZP	UHF-DZP	UMP2-DZP
Total energies	−187.979260	−188.568775	−187.956789	−188.553157
Zero-point energies	0.080223	0.078516	0.079834	0.079939
d(N–C)	2.283	2.164	2.244	2.098
Imag. freq. sym. C–N strech.	663i	550i	867i	782i
Imag. freq. asym. C–N strech.	146i	114i	326i	354i
Barrier heights without ZPE	49.2	64.7	50.6	64.2
Barrier heights with ZPE	43.6	59.5	45.1	48.9

several additional structures along the reaction path were first optimized at the UHF/DZP level by fixing the elongated d(C–N) bond length and minimizing the energy profile yielding an adequate initial guess for the Berny algorithm. The localized transition structures, having one imaginary frequency which correspond to the asymmetric C–N stretching mode, were accompanied by large spin contamination, (i.e. $\langle S^2 \rangle = 1.53$). After projection of the spin contaminants these barriers disappeared, and only smoothly increasing potential curves were revealed. Therefore, the dissociation energies were determined from total energies of reactants and products. The results of these calculations are summarized in Tables 1, 6 and 7. The computed dissociation energies D_0 of *cis*- and *trans*-isomer at the SCF level within TZ2P basis including the zero-point corrections are 30.9 and 19.3 kcal/mol, respectively. The dissociation energies predicted with inclusion of correlation effect are significantly larger than those obtained at the SCF level. At the PMP4SDTQ/TZ2P//UMP2/TZ2P level the predicted D_0 for *trans*-azomethane is 47.8 kcal/mol which is by 4 kcal/mol lower than the experimental value 51.2 kcal/mol published by Steel and Trotman-Dickenson [29, 30].

It is well known that energies obtained by annihilation only of the next highest spin are not size consistent [13]. To eliminate this discrepancy and the basis set superposition error (BSSE), we calculated the total energies of *trans*-azomethane for d(C–N) = 5 and 10 Å, respectively. The difference of energies for these bond lengths was negligible, only 0.125 kcal/mol, indicating that obtained values reproduce very well the asymptotic product region. Thus, the corrected dissociation energy of *trans*-azomethane was by 1.3 kcal/mol above the value calculated by the other way, namely as the difference of total energies of products and reactant.

A final improvement of the dissociation energy requires some explanation. Since quantum chemical calculations generally underestimate stabilization energy accompanying electron pairing, these calculations are most successful for isogyric energy comparison, i.e. for comparisons between molecules having the same number of electron pairs. The dissociation of molecule into radical products is not

Table 6. Predicted equilibrium geometries and zero-point energies (in hartrees) for products with bond lengths in angstroms and bond angles in degrees

	UHF		UMP2	
	DZP	TZ2P	DZP	TZ2P
CH_3–N_2^*				
Zero-point energies	0.053615	0.053365	0.053122	0.053303
R_{12}	1.168	1.152	1.182	1.160
R_{23}	1.475	1.480	1.486	1.493
R_{43} R_{53}	1.082	1.078	1.092	1.080
R_{63}	1.083	1.078	1.089	1.079
a_{321}	119.8	119.4	120.5	120.3
a_{432} a_{532}	108.5	109.2	109.0	110.2
a_{632}	111.2	110.7	114.3	111.6
CH_3^*				
Zero-point energies	0.028309	0.028654	0.027361	0.027534
R_{12} R_{13} R_{14}	1.075	1.067	1.078	1.075
a_{312} a_{412} a_{413}	118.7	119.2	120.6	120.1

R_j – distance between atoms i and j (bond lengths)
a_{ijk} – angle between atoms i, j and k (bond angles)

Table 7. Calculated dissociation energies (in kcal/mol) for asynchronous reaction pathway (*cis*- and *trans*-azomethane)

	trans		*cis*	
D_e	D_e	D_0	D_e	D_0
UHF/DZP	37.6	33.5	24.9	20.7
UHF/TZ2P	34.8	30.9	23.4	19.3
UMP2/DZP	51.4	47.8	41.1	37.2
PMP2/DZP[a]	35.4	31.8		
UMP2/TZ2P	49.6	46.3	39.8	36.3
PMP4/TZ2P[b]	51.2	47.8	41.8	38.5
PMP4/TZ2P[c]		49.1		
PMP4/TZ2P[d]		54.0		
Experiment[e]		51.2 kcal/mol		

[a] Only the next highest spin state was annihilated
[b] ZPE corrections obtained at UMP2/TZ2P level were used
[c] ZPE correction obtained at UMP2/TZ2P level was used and energy of products was calculated for d(N–C) bond distance 10 Å.
[d] as in b, moreover, the Truhlar's correction was used – see text
[e] Ref. [29]

isogyric, and thus quantum chemical methods usually underestimate bond energies. For example, Gordon and Truhlar [31] presented MP4/6-311G** bond dissociation energies for a large number of dissociations in the form $XH_mYH_n \rightarrow XH_m^* + YH_n^*$, where X and Y were first row atoms and m and n chosen so that the

molecule was fully saturated with hydrogens. They found that single-bond dissociation energies are underestimated by: N–N 6.8 kcal/mol, O–O 7.7 kcal/mol, C–C 1.6 kcal/mol, C–O 5.5 kcal/mol and C–N 4.9 kcal/mol, respectively. Provided that the unrestricted Hartree–Fock reference wave function insures a reasonable description of the bond dissociation process, according to the above discussion, and the MP4/6-311G** C–N bond dissociation error of 4.9 kcal/mol for CH_3NH_2, our C–N bond dissociation energy in *trans*-azomethane with a similar basis set might be expected to be low by about 5 kcal/mol. Based on our best calculation, and the present discussion, we estimate the C–N bond dissociation energy in *trans*-azomethane to be 54.0 kcal/mol.

The potential energy curve (PEC) for *trans*-azomethane was calculated as described in Sect. 2. The poor agreement obtained with the MP2/DZP reaction path means that we have to reoptimize our *ab initio* potential surface. Figure 2 illustrates the calculated PECs at three levels of theory, PMP2/DZP, UMP4/TZ2P and PMP4/TZ2P. With respect to the experimental barrier of the decomposition, the PMP2/DZP level is the lower limit, but this value grows up drastically if fourth-order correlation is included. The spin annihilation affects mostly the shape of the dissociation curve.

From the above analysis, we can conclude that the inclusion of the correlation energy at very accurate method with large basis set does not provide the correct experimental dissociation limit. In order to obtain canonical variational rate constants that are comparable with experiment it is necessary to calibrate the calculated PEC. Note that this calibrations produced a substantial change in the shape of the curve which will affect the kinetic results. In the following, we propose various methods of calibration.

Method 1: To increase the height of the barrier, the PMP2/DZP curve was scaled up regularly by factor

$$F = \frac{E(\text{PMP4/TZ2P} + \text{corr.}, r = \infty)}{E(\text{PMP2/DZP}, r = \infty)},$$

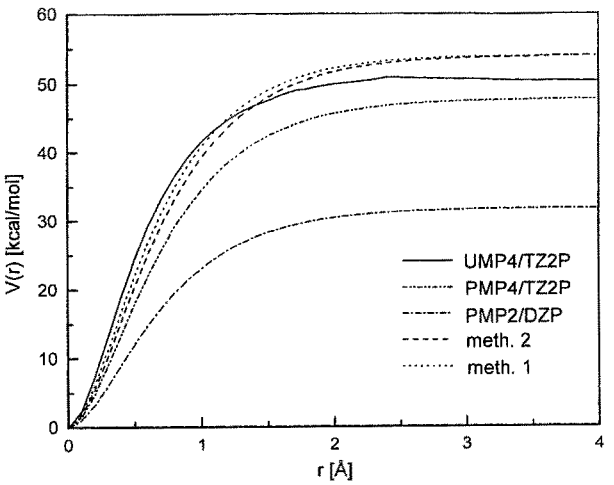

Fig. 2. Potential energy curves calculated at several levels. (The relative energies are calculated with respect to the *trans*-azomethane in equilibrium, zero-point energies are included too)

where E(PMP4/TZ2P + corr., $r = \infty$) is the corrected PMP4/TZ2P barrier height (see Table 7, case c) and E(PMP2/DZP, $r = \infty$) is the same for PMP2 level.

Method 2: It was shown by Hase et al. [32] that the variationally localized rate coefficient is quite sensitive to the assumed form for $V(r)$. In order for the shape of the original curve to be conserved, the calculated PMP2/DZP curve was fitted to the Morse function

$$V(r) = D_e(1 - e^{-\beta r})^2.$$

The β parameter obtained from fitting ($\beta = 1.875$ Å^{-1}) was used to determine the scaled potential energy curve, where $D_e = 54$ kcal mol^{-1} was used in the Morse function.

3.5 RRKM results

In order to further investigate the possible mechanism in relation to the observed kinetics for *trans*-azomethane, the RRKM calculations were performed for this system [33]. It was shown previously that the asynchronous pathways do not have a saddle point on the reaction coordinate. Therefore, it is very important to determine the position of the transition state variationally. Because canonical variational calculations are temperature-dependent, minimization of high-pressure unimolecular rate coefficients was performed at temperature $T = 603$ K, which was used in the experiment [29].

The absolute magnitude of the variationally established rate coefficients depends critically on the calculated values for the energy threshold and on the shape of the interaction potentials. In our calculations, the two scaled potential energy curves were used with Morse parameters $D_e = 54.0$ kcal/mol and $\beta = 1.875$ Å^{-1} (Method 1) and $D_e = 54.0$ kcal/mol and $\beta = 2.017$ Å^{-1} (Method 2), respectively. This value of critical energy produces activation energy $E_a = 52.4$ kcal/mol at $T = 603$ K which is only by 1.2 kcal/mol above the experimental activation energy.

In treating the loose transition state, we make the assumption, implicit in the Gorin model [34], that the vibrational frequencies of the fragments in the transition state are the same as in the completely separated products. We take the scaled MP2/TZ2P frequencies as given in Table 3.

Canonical variational selection of the transition state involves the evaluation of moments of inertia for a range of different separations of fragments. In these calculations, the rocking motions of fragments were treated as steric hindrance two-dimensional rocking modes. This model should be most useful at lower temperatures, where the transition state chosen by canonical variational methods lies at larger separations of moieties. The results of RRKM calculations, which were carried out by means of the UNIMOL program package [35], are shown in Fig. 3. The variation of the predicted high-pressure rate coefficient as a function of the separation r of the moieties in the transition state gives results which illustrate the behaviour expected in any variational transition state calculation. The shallowness of the minimum is probably the result of the assumption that the fragments in the loose transition state are product-like, and do not change in the vibrational frequencies with r. For this model therefore the enthalpic effect (shape of the Morse curve) tends to dominate the positioning of the transition state. The predicted rate coefficients support this hypothesis. The values obtained by canonical variational method are $k_{uni}^{\infty} = 2.8 \times 10^{-5}$ s^{-1} ($\beta = 1.875$ Å^{-1}) and $k_{uni}^{\infty} = 3.2 \times 10^{-5}$ s^{-1} ($\beta = 2.017$ Å^{-1}), respectively, at $T = 603$ K. The experimental value $k_{uni}^{\infty} =$

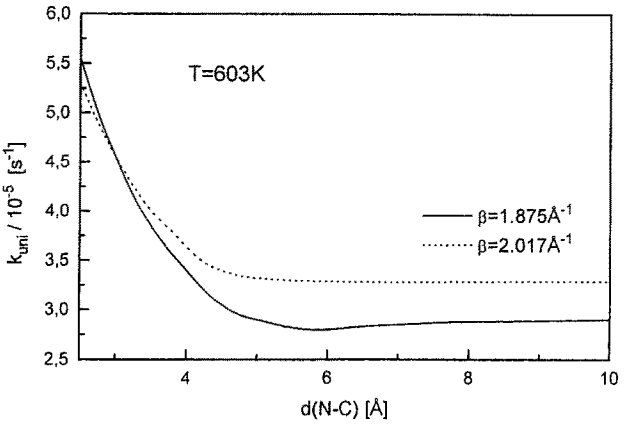

Fig. 3. Canonical variational calculation for the decomposition of *trans*-azomethane within loose transition state model at $T = 603$ K. Plot shows the variation of the predicted high-pressure rate coefficient from the separation of fragments r

$2.25 \times 10^{-5}\,s^{-1}$ reflected that the interaction potential between fragments in decomposition of *trans*-azomethane have a long-range character (smaller β parameter). The temperature-dependent calculation for $\beta = 1.875\,Å^{-1}$ in the range of temperature from 300 to 800 K gives the result

$$\log k_{\text{uni}}^{\infty} = 16.27 - \frac{1}{2.303}\frac{52.96}{RT},$$

which is in reasonable agreement with the experiment.

4 Conclusions

In the present work the features of the potential energy surface pertinent to the thermal decomposition mechanism of *cis*- and *trans*-azomethane were investigated by Hartree–Fock (UHF) and Møller–Plesset molecular orbital methods. At issue are the activation energies both for synchronous dissociation leading to CH_3 and N_2 and for the simple N–C bond cleavage leading to $CH_3N_2^{\bullet}$ and $CH_3^{\bullet}$. It was established that synchronous transition states (which are second-order saddle points, and not the true transition states) lie by 13 kcal/mol above the asynchronous transition states. Hence, the decomposition proceeds by a two-step reaction mechanism.

The scaled vibrational frequencies calculated at the MP2 level using TZ2P basis set are in good agreement with the experiment, and agree exceptionally well for vibration modes over 900 cm^{-1}.

In the case of asynchronous decomposition, the dissociation energy for *cis*-azomethane is by 9.3 kcal/mol lower than that for *trans*-azomethane. This fact suggests that the gas-phase two-step decomposition of more stable *trans*-azomethane proceeds via a *cis*-transition state. However, the experimentally established value is nearer to the value calculated for the *trans*-azomethane, which means that the barrier to *trans–cis* isomerization is probably higher than the barrier height to the decomposition of the *trans*-azomethane.

As the theoretical results underestimate the experimental activation energies and overestimate the rate coefficient, we analyzed a sequence of possible improvements to the potential energy curve and vibrational frequencies. Although the introduction of a major correlation energy with MP4 method increases the barrier by 16.9 kcal/mol with respect to the Hartree–Fock calculation, it is necessary to scale parameters to experimental values in order to obtain reasonable agreement with the experiment. This problem raises some interesting questions. For a system for which experimental data are lacking or have large error margins, the question that which method should be chosen to scale the parameters remains still open.

References

1. Porter NA, Marnett LJ, Lochmüller CH, Closs GJ, Shobataki M (1972) J Am Chem Soc 94:3664
2. Ramsperger HC (1929) J Am Chem Soc 51:2134
3. Burton KA, Weismann RB (1990) J Am Chem Soc 112:1804
4. Miller JA, Branch MC, Kee RJ (1981) Combust Flame 90:1624
5. Holt PL, McCurdy KE, Adams JS, Burton KA, Weisman RB, Engel PS (1985) J Am Chem Soc 107:2180
6. North SW, Longfelow CA, Lee TY (1993) J Chem Phys 99:4423
7. Dannenberg JJ, Rocklin D (1982) J Org Chem 47:4529
8. Hu CH, Schaefer III HF (1995) J Phys Chem 99:7507
9. Frisch MJ, Trucks GW, Schlegel HB, Gill PMW, Johnson BG, Wong MW, Foresman JB, Robb MA, Head-Gordon M, Replogle ES, Comperts R, Andres JL, Raghavachari, Binkley JS, Gonzales C, Martin RT, Fox DJ, Defrees DJ, Baker J, Stewart JJP, Pople JA (1993) Gaussian 92, Gaussian, Inc., Pittsburgh PA, 1993
10. Schlegel HB (1982) J Comp Chem 3:214
11. Saxe P, Yamaguchi J, Schaefer III HF (1982) J Chem Phys 77:5674
12. Schlegel HB (1994) J Chem Phys 101:5957
13. Schlegel HB (1986) J Chem Phys 84:4530
14. Seeger S, Pople JA (1977) J Chem Phys 66:3045
15. Huzinaga S (1965) J Chem Phys 42:1293
16. Dunning TH (1971) J Chem Phys 55:716
17. Stevens JF, Curl JF, Engel PS (1979) J Phys Chem 83:1432
18. Flood E, Pulay P, Boggs JC (1978) J Mol Struc 50:355
19. Haaland A, Almenningen A, Anfinsen IM (1970) Acta Chem Scand 24:1230
20. Chang CH, Porter RF, Bauer SH (1970) J Am Chem Soc 92:5313
21. Craig MC, Ackermann MN, MacPhail RA (1978) J Chem Phys 68:276
22. Pearce AR, Lewin IW, Harris WC (1973) J Chem Phys 59:1206
23. During JR, Pate CB, Harris WC (1972) J Chem Phys 56:5652
24. Ackermann MN, Craig NC, Isberg RR, Lauter DM, Tacy EP (1978) J Phys Chem 83:1190
25. Ackermann MN, Craig NC, Isberg RR, Lauter DM, MacPhail RA, Young WG (1977) J Am Chem Soc 99:1661
26. Hehre W, Random L, Schleyer P, Pople JA (1986) *Ab initio* molecular orbital theory. Wiley, New York
27. Zubkov VA, Yakimansky AV, Bogdanova SE (1993) J Mol Struc (Theochem) 306:269
28. Grodzicki M, Seminario JM, Politzer P (1990) Theo Chim Acta 77:359
29. Steel C, Trotman-Dickenson AF (1959) J Chem Soc 975
30. Engel PS (1980) Chem Rev 80:99 and references therein
31. Gordon MS, Truhlar DG (1986) J Am Chem Soc 108:5412
32. Duchovic RJ, Hase WL (1985) J Chem Phys 82:3599
33. Gilbert RG, Smith SC (1990) Theory of unimolecular and recombination reactions. Alden Press, Oxford
34. Gorin E (1938) Acta Physiochim 9:691
35. UNIMOL program Gilbert RG (1990)